Exploring and selecting supershapes in virtual reality with line, quad, and cube shaped widgets

Exploring and Selecting Supershapes in Virtual Reality with Line, Quad, and Cube Shaped Widgets

Francisco Nicolau*
Instituto Superior Técnico
University of Lisbon

Johan Gielis †
Department of
Biosciences Engineering
University of Antwerp

Adalberto L. Simeone ‡
Department of
Computer Science
KU Leuven

Daniel Simões Lopes §
INESC-ID
Instituto Superior Técnico
University of Lisbon

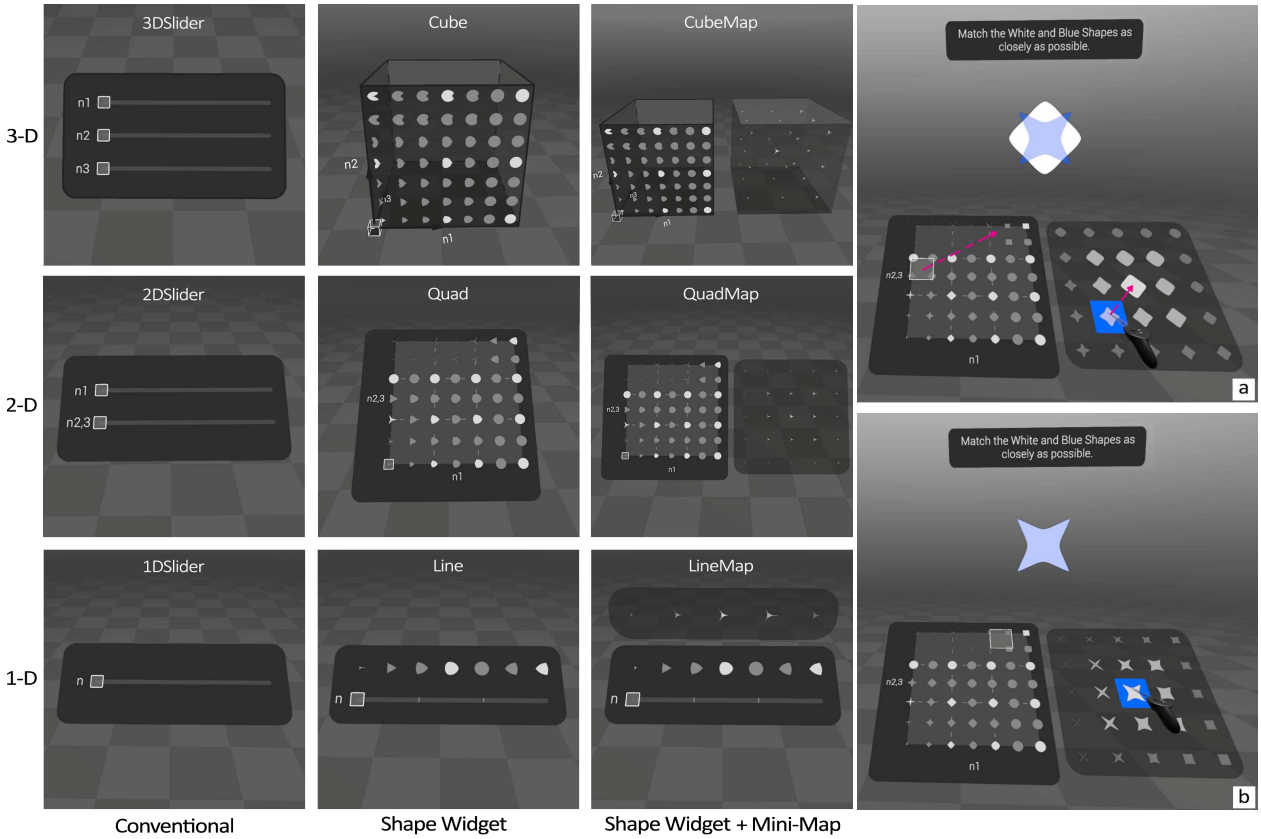

Figure 1: On the left-side, VR shape widgets for exploring and selecting supershapes. On the right-side, a selection task example for which a user starts adjusting a handle (a) to match a target shape (b).

Abstract

Supershapes are used in Parametric Design to model, literally, thousands of natural and man-made shapes with a single 6 parameter formula. However, users are left to probe such a rich yet dense collection of supershapes using a set of independent 1-D sliders. Some of the formula's parameters are non-linear in nature, making them particularly difficult to grasp with conventional 1-D sliders alone. VR appears as a promising setting for Parametric Design with supershapes since it empowers users with more natural visual inspection and shape browsing techniques, with multiple solutions being displayed at once and the possibility to design more interesting forms of slider interaction. In this work, we propose VR shape widgets that allow users to probe and select supershapes from a multitude of solutions. Our designs take leverage on thumbnails, mini-maps, haptic feedback and spatial interaction, while supporting 1-D, 2-D and 3-D supershape parameter spaces. We conducted a user study ($N = 18$) and found that VR shape widgets are effective, more efficient, and natural than conventional VR 1-D sliders while also usable for users without prior knowledge on supershapes. We also found that the proposed VR widgets provide a quick overview of the main supershapes, and users can easily reach the desired solution without having to perform fine-grain handle manipulations.

Index Terms: Human-centered computing—User interface design; Human-centered computing—Virtual reality Human-centered computing—Graphical user interfaces

1 Introduction

Parametric Design (PD) represents objects as a collection of shapes with well-defined parameters that encode geometric features such as dimension, curvature or symmetry [11]. These shapes can be

*e-mail: francisonicolau@tecnico.ulisboa.pt
†e-mail: johan.gielis@uantwerpen.be
‡e-mail: adalberto.simeone@kuleuven.be
§e-mail: daniel.lopes@inesc-id.pt

changed by modifying parameter values, thus, allowing users to easily generate a large and diverse number of objects from a single formula or algorithm. Supershapes are a class of parametric models used in PD to represent a plethora of natural and man-made shapes [26, 27, 47]. PD with supershapes has been studied before in curve/surface fitting [49], computer vision [23], Constructive Solid Geometry [20, 22], shape recovery [21], and even procedural modeling in Virtual Reality (VR) [37]. In fact, several real-world applications rely on PD with supershapes such as designing or modeling urban buildings [37], tangible user interfaces [33], wind turbines [44], antennas [8], seed morphology [48], nanotechnology [6], mechanical design [12, 13], robotic haptic recognition [24] among many other examples.

Many VR apps for PD exist [1, 4, 9] and several studies have reported that PD benefits from VR as immersive technologies promote the creation of 3-D shapes in different design stages [15, 17, 19]. Surely, VR can also become an appropriate medium for modeling objects made of supershapes. Actually, 2-D supershape apps are already available in game engine asset stores such as [3] but studies on VR applied to PD with supershapes are still lacking [37].

Probably the most obvious VR scenario for PD with supershapes is to explore and select smooth curved objects within the parameter space. Supershapes were originally formulated to model objects found in nature such as eggs, flowers, leaves, shells or horns [26, 30]. Yet, in VR, such organic objects are commonly modeled with polygonal meshes [43] or splines [2, 46] that, although more flexible for designing smooth curved objects, carry a lot of manual input in the form of sketching multiple strokes and editing many control points. Supershapes could complement these 3-D modeling tasks by providing 2-D cross-section curves or 3-D shapes of entire objects that could easily be converted into polygonal meshes [42] and even spline curves [12].

However, interacting with supershapes comes with a couple of challenges. Firstly, users are left to probe such a rich yet dense collection of supershapes using conventional 1-D sliders, leaving users to fiddle and tweak the numerical values of the parameters by adjusting slider handles [18, 35, 39, 40]. Secondly, some of the formula's parameters are non-linear in nature, making them particularly difficult to grasp with conventional 1-D sliders alone. Such supershape challenges were partially addressed by Lopes et al. [39] who proposed two widgets for supershape exploration and selection comparing them to 1-D sliders in terms of task completion, selection accuracy and user satisfaction. However, their study considered flat WIMP interfaces that are well known to hinder the process of visual exploration and shape selection. This creates an opportunity to re-frame supershape widget design in the context of VR. In fact, VR appears as a promising medium to address these challenges since it empowers users with more natural visual inspection and shape browsing techniques, making multiple solutions available at once and the possibility to design more interesting forms of slider interaction [10, 34, 38].

Therefore, before developing a fully fledged VR system for PD with supershapes, it is necessary to address which type of VR widgets best suit fundamental supershape modeling tasks. According to Bowman et al. [10], selection is a generic task to any 3D user interface. This of course applies to PD in VR. Moreover, not only VR can make available dozens or hundreds of shape solutions at once, but empowers users with camera control, bi-manual interaction and body movements that promote more natural visual inspection, shape browsing and shape selection tasks [34]. Thus, to promote VR as a medium for PD with supershapes, it is necessary to first design widgets suitable for probing and selecting supershapes from a multitude of solutions.

In this work, we propose VR widgets shaped as lines, quads, and cubes to explore and select supershapes from 1-D, 2-D, and 3-D parameter spaces. Each parameter space is a sub-set defined by the three non-linear parameters of the supershape formula. Our widget design options are based on guidelines from the literature that inform which widget features make parameter space exploration more user-friendly [5, 7, 34, 38, 41]. In particular, our designs take leverage on thumbnails, mini-maps, haptic feedback and spatial interaction, while supporting 1-D, 2-D, and 3-D supershape parameter spaces. We conducted a user study to evaluate whether the proposed VR shape widgets support a more natural probing and selection of supershapes, and verify if they have adequate usability for users that have no prior knowledge on supershapes. We compare the VR shape widgets among each other and against conventional 1-D sliders. Task completion time, selection accuracy, perceived usability and task load, participant satisfaction and participant preferences were measured to validate our initial concepts of the line, quad, and cube VR shape widgets (Figure 1).

2 Supershapes

Also known as Gielis Transformations [27,47], supershapes have the noteworthy capacity to model a rich family of natural and man-made 2-D shapes, while relying only on a single mathematical formula with just 6 or less parameters [26]. Supershapes have even been successfully tested on more than 40000 specimen from biology [30]. More complex 3-D shapes can be modeled with two or more 2-D supershapes either by applying a cross-product between a pair of orthogonal supershapes or by defining the cross-sections of a generalized cylinder as supershapes [27].

In computer graphics, supershapes were introduced as a generalization of superquadrics [28, 29], but can also be considered as the generalization of polygons with linear or non-linear curved edges, i.e., supershapes are able to represent a variety of symmetrical and asymmetric shapes with either smooth boundaries or sharp features. The geometric locus of a supershape is defined by its relative dimensions (a, b), number of sides (m), and three exponents (n_1, n_2, n_3) whose non-linear behaviour regulates the curvature of the sides, i.e., define a more convex or concave shape appearance. The 2-D supershape formula is written in the following parametric angle-center expression:

$$r(\theta) = \left(\left| \frac{\cos(\frac{m}{4}\theta)}{a} \right|^{n_2} + \left| \frac{\sin(\frac{m}{4}\theta)}{b} \right|^{n_3} \right)^{-\frac{1}{n_1}} \quad (1)$$

where $r \in \mathscr{R}_0^+$ and $\theta \in [0, 2\pi[$ are the polar coordinates of radius and angle, respectively. Figure 2 showcases several types of supershapes with varying a, b, m, n_1, n_2, and n_3. Given the 6 parameters of (Equation 1), the exponents n_1, n_2, and n_3 are those that spark greater interest. While a, b, and m are intuitive parameters (i.e., they define the size and number of sides of the shape), the exponents have a non-linear behaviour.

To cope with the challenges of interacting with the non-linear and multi-dimensional parameter space defined by the exponent values, we propose the design of line, quad, and cube shaped widgets for probing 1-D ($n_1 = n_2 = n_3$), 2-D ($n_1 \neq n_2 = n_3$), and 3-D ($n_1 \neq n_2 \neq n_3$) exponent parameter spaces, respectively. Several studies only consider such sub-sets of the exponent parameter space (i.e., $n_1 = n_2 = n_3$; $n_1 \neq n_2 = n_3$) since the full set (i.e., $n_1 \neq n_2 \neq n_3$) is vast and often does not offer many useful shape solutions [27, 30]. Moreover, since these sub-set exponent parameter spaces are more constrained they offer greater control for exploration tasks and to find a desirable shape solution. Nevertheless, the full set can be also of interest, in particular, for providing more creative or exotic shape solutions that cannot be found in the sub-sets, which is particularly useful for computational creativity applications [16].

3 Supershape Line, Quad, and Cube Widget Design

A total of 6 shape widgets were designed to explore and select supershapes from 1-D, 2-D, and 3-D exponent parameter spaces

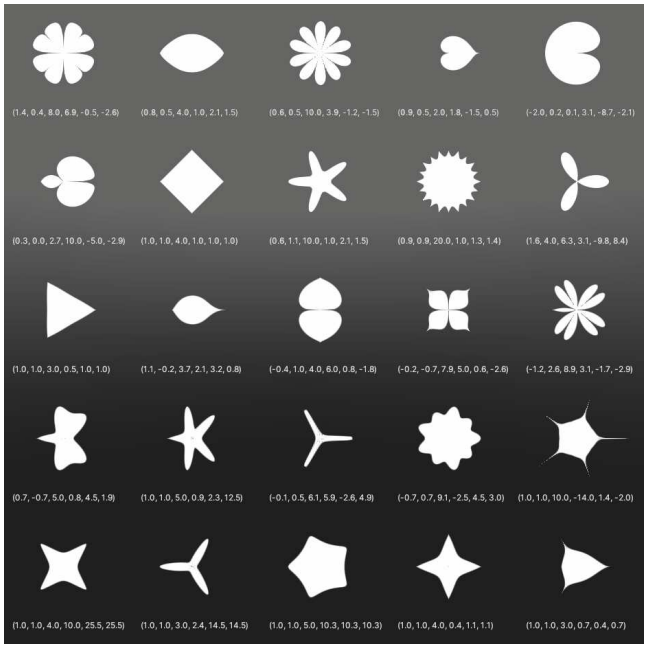

Figure 2: Assortment of supershapes with different dimensions (a,b) values of number of sides (m) and exponents (n_1,n_2,n_3). Each underlying array corresponds to (a,b,m,n_1,n_2,n_3).

(Figure 1). Our supershape widgets consider techniques found in slider design and infovis studies [7, 32, 38, 41]. Even though most of these techniques were not designed with VR in mind, they are easily extendable to spatial user interfaces [5, 34]. The implemented techniques were the following:

Re-scaling - Since most of the supershapes' diversity resides in exponent values that belong to sub-intervals $]0,1]$ and $]1,2]$ [27], we re-scaled the exponent parameters so that the sub-intervals $n_i \in]0,1],]1,2]$ and $]2,L]$ $(i = 1,2,3,\ L \in \mathscr{R}^+, L \gg 2)$ had the same length/area/volume in the sliders tracks (Figure 3). Without loss of generality, we consider non-null positive exponents only.

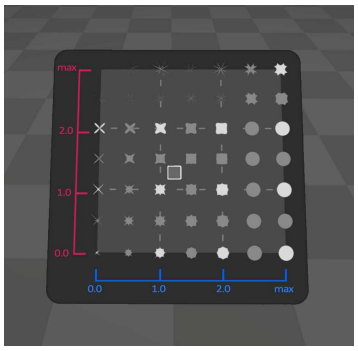

Figure 3: A quad widget showcasing equally spaced sub-intervals of the exponent values.

Thumbnails - Liu et al. [38] explored small multiples to display a great variety of design solution at once, to facilitate visual comparisons and provide an overview of the data with minimal interaction. Here, we replace the concept of 'small multiples' with thumbnails, each of which represents a supershape placed at equally spaced positions within the re-scaled intervals (i.e., $n_i \in \{0^+, \frac{1}{2}, 1, 1\frac{1}{2}, 2, \frac{L}{2}, L\}$, where $L \gg 2$), which guarantees a proper sampling of these intervals without loss of details [27, 42]. Each thumbnail is clickable to enable users to select the displayed supershape. All the considered thumbnail layouts follow the traditional arrangement of a grid with a fixed and predefined order (Figure 4) [38]. For the cube shaped widget (Figure 4(c)), we followed the Space Cutting technique by Bach et al. [7]. Although this method does not show an overview of the entire space at once, it does significantly reduce visual noise and can be used to quickly survey the entire cube in one continuous motion.

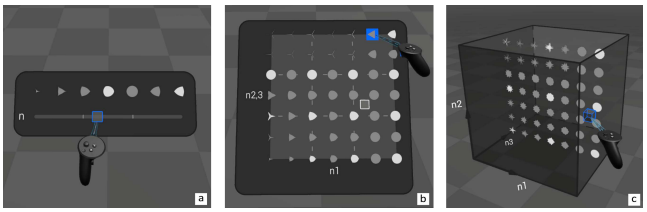

Figure 4: Three types of VR shape widgets picturing thumbnails for (a) 1-D, (b) 2-D, and (c) 3-D exponent parameter spaces.

Bands - Sliders of continuous value benefit from representing sub-intervals with bands instead of ticks [41]. The usage of bands to decorate a slider enables unbiased handle adjustments with the precision of tick marks while reducing response time. Thus, bands were used to visually represent the span of each exponent sub-interval.

Mini-maps and re-sizable handles - Similar to a World-in-Miniature [7, 14], we also considered mini-maps that display regular spaced samples of supershapes in the vicinity of the handle position, which inform the user about the supershapes underlying the area occupied by the slider handle (e.g., a smaller handle represents a smaller sub-interval), consequently, allows for more precise fine-tuning. More specifically, whenever a handle, placed at exponent value v, is re-sized to a width w, the mini-map showcases multiples of 3 (i.e., $n_i \in \{v - \frac{w}{2}, v, v + \frac{w}{2}\}$) or 5 (i.e., $n_i \in \{v - \frac{w}{2}, v - \frac{w}{4}, v, v + \frac{w}{4}, v + \frac{w}{2}\}$) thumbnails per parameter dimension (Figure 5).

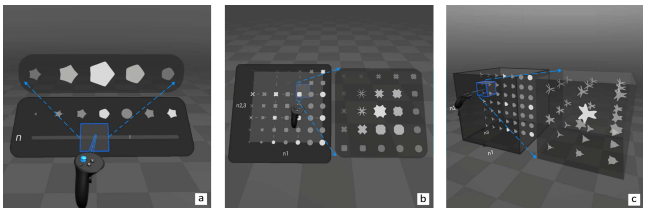

Figure 5: Three types of VR shape widgets picturing mini-maps and re-sizable handles for (a) 1-D, (b) 2-D, and (c) 3-D exponent parameter spaces.

Haptic feedback - Tactile haptics in the form of vibration is considered a supporting channel that enhances the visual feedback of touch during manipulation tasks [45]. Therefore, subtle haptic feedback (i.e., small intensity and short duration pulses) was introduced whenever the handle reaches key points of the exponent parameters space (i.e., $n_i \in \{0^+, \frac{1}{2}, 1, 1\frac{1}{2}, 2, \frac{L}{2}, L\}$). Note that haptic feedback was not used when selecting thumbnails, but just to inform the user whenever the handle reached an end point or crossed over the sub-intervals of the exponent values.

3.1 VR 1-D Sliders

As baseline of comparison, for each dimension we consider a set of 1 (*1DSlider*), 2 (*2DSlider*) and 3 (*3DSlider*) 1-D sliders vertically

stacked inside a panel (Figure 1). Such sliders follow their counterpart 2-D desktop metaphor to perform numerical value adjustments. The exponents of the supershape formula are directly mapped to these sliders. Interaction with 1-D sliders can be done by moving a handle constrained to a track or clicking on a point on the track.

3.2 Supershape Line Widgets ($n_1 = n_2 = n_3$)

Two line shaped widgets (*Line* and *LineMap*) were designed to select shapes inside a 1-D exponent parameter space and have a similar mechanics to traditional 1-D sliders (Figure 1). They only allow the input of a single value $\gamma = n_1 = n_2 = n_3$ encoded by the coordinate of the handle relative to the origin of the track (left end). These widgets have three distinct bands and haptic feedback to denote when the user transitions from one band to another. It features an array of 7 thumbnails. Similarly, the mini-map for *LineMap* shows an array of 5 shapes being sampled from the sub-interval defined by the handle, presented in a separate panel above the slider.

3.3 Supershape Quad Widgets ($n_1 \neq n_2 = n_3$)

As for the 2-D exponent parameter space, we designed two quad shaped widgets (*Quad* and *QuadMap*) represented by square handles that move within square tracks forming 2-D sliders (Figure 1). They allow two input values respectively encoded by the x and y coordinates of the handle relative to the origin of the track (lower left corner). The resulting shape is dictated by $\gamma_1 = n_1$ and $\gamma_2 = n_2 = n_3$. The tracks are divided into 3×3 re-scaled bands and haptic feedback is provided to indicate transitions between bands. They feature an embedded matrix of 7×7 thumbnails. Likewise, *QuadMap* has a secondary panel or mini-map, positioned to the right of the slider that shows a matrix of 5×5 thumbnails sampled from the sub-interval inside the handle.

3.4 Supershape Cube Widgets ($n_1 \neq n_2 \neq n_3$)

Regarding the 3-D exponent parameter space, we designed two cube shaped widgets (*Cube* and *CubeMap*) represented by cubic handles with cube-shaped tracks forming 3-D sliders (Figure 1). Both support three input values respectively encoded by the x, y and z coordinates of the handle relative to the origin of the track (lower left corner of the cube's closest face). The user can control all three exponent parameters. The resulting shape is dictated by $\gamma_1 = n_1$, $\gamma_2 = n_2$ and $\gamma_3 = n_3$. Inside the cube, 2-D slices are populated by thumbnails in the same configuration as the *Quad* widget. Sliding the handle along the z axis of the cube, shows a forward-facing 2-D slice of the 3-D parameter space encompassed by the slider's track similar to a color cube [34]. The mini-map of *CubeMap* is a 3-D matrix of 3×3 thumbnails representing the sub-interval of the slider handle; this number is more reduced than it's lower dimensional counterparts due to excessive overlap in primitives which made it too cluttered to use efficiently.

4 User Study

A user study was conducted to assess supershape selection performance, perceived usability, perceived task load, user satisfaction and preferences of the proposed VR shape widgets. We declare the type of VR widget as our single independent variable (*WidgetDesign*): conventional 1-D sliders (*1DSlider*, *2DSlider*, *3DSlider*), shape widgets without mini-map (*Line*, *Quad*, *Cube*), and shape widgets with mini-map (*LineMap*, *QuadMap*, *CubeMap*). To address the research questions of our study, we declare 4 dependent variables: (i) Task Completion Time, (ii) Selection Error, (iii) Perceived Usability, and (iv) Perceived Task Load. Note that, we are interested in assessing the metrics per parametric space dimension and not between different dimensions.

We consider the following hypothesis for our study:

H1: Shape widgets will produce shorter task completion times.

H2: Shape widgets will contribute towards smaller selection error.

H3: Including a Mini-Map will increase the accuracy of the selections.

H4: Shape widgets will produce a higher perceived workload.

H5: Shape widgets will generally be perceived as having better usability.

4.1 Participants

A total of 18 volunteer participants performed the user study (26.3 ± 7.9 years old, 7 female). Recruitment was done through email lists for people interested in participating in Human-Computer Interaction studies. Nine participants had hobbyist level of experience while one operates shape modeling software in a daily basis. Regarding their experience with VR, eight have a high level of VR experience (level of expertise 4 in 1-5 scale; 5 indicates full agreement) while the remaining participants had little to none VR experience. None of the participants indicated to be familiar to supershapes (1 in a 1-5 scale; 5 indicates full agreement), in fact, none of them knew what a supershape was before the experiment.

4.2 Apparatus

Our setup relies on the Oculus Quest™ headset. Both controllers were used as hand-held input devices to track hand gestures, to provide button input and to render haptic feedback. All code development was performed using Unity (v2020.2), XR Interaction Toolkit (v0.9.4) and C# scripting. Supershapes were rendered with an in-house HLSL fragment shader.

4.3 Measures

We measured the following dependent variables:

Task Completion Time (TCT) [seconds]. The time taken by the user to complete a given task. The time is counted from the moment the target shape is presented to the moment the user decides they are satisfied with the result.

Selection Error (SE) [exponent difference value]. The absolute difference between the selected exponent and the corresponding target exponent (three exponents are calculated per task). For the purpose of analysis, we average the relevant exponent errors for each dimension level.

System Usability Scale (SUS) [score 0-100]. Simple, reliable tool for measuring perceived usability.

Task Load Index (Raw NASA-TLX) [score 0-100]. Subjective, multidimensional rating procedure to determine perceived workload and assess a system's effectiveness. The sub-scales were not rated by participants and were considered to be equally weighted [31].

4.4 Tasks

Participants were invited to perform habituation tasks that consisted of interacting with all available features, introducing participants to supershapes and enabling them to explore the parameter space values. A total of 9 habituation tasks (1 per widget) were performed. Then, participants were asked to select a shape that matched, as closely as possible, a target shape displayed in front of them (Figure 1). Participants were prompted to complete 27 tasks (3 exponent parameter spaces x 3 VR shape widgets per parameter space x 3 target shapes). All target shapes differed from each other, none consisted of a common shape (e.g., circle or regular polygon) nor was any of the target shapes one of the displayed thumbnails. Without loss of generality, target shapes parameters were defined with relative dimensions $a, b \in \mathscr{R}^+$, number of sides $m \in \mathscr{N}_0$, and exponents $n_1, n_2, n_3 \in]0, 50]$. Each task session was individual and timed, although a time limit of 90 seconds was imposed. Besides the controls of each VR shape widget, the participant had a 'done' button to set

the TCT, which was measured since the beginning of the task until the participant was satisfied with the result.

4.5 Procedure

Each session was conducted remotely as we could not perform the experiments in a laboratory environment due to COVID-19 restrictions. Participants were asked to download the application and install it on their own Oculus Quest. The study procedure was completely scripted and ran without the oversight of an experimenter. All questionnaires were online forms presented directly in VR (Oculus Browser) using a readable font size. In terms of experimental setting, each participant wore a headset, held both controllers on each hand and were instructed to perform the study in standing position in a room without nearby obstacles nor distractions. The relative positions and orientations of the avatar and all VR content was determined by Oculus Quest tracking system. The widgets were placed in front of the participant at arm's reach, with the panels placed at a 45° inclination bellow shoulder height so that the panels are faced towards the user's head. The size of the sliders, handles and panels lie within ranges of found in real-world controls and VR widgets [5].

The expected duration of each evaluation session was about 30-45 minutes. Before performing any task, participants were prompted to fill in an Informed Consent and Demographic Profile forms. Afterwards, participants were guided through the interactive system. Then, they were asked to explore the widgets to familiarize themselves with the interface and its mechanics followed by the execution of 27 tasks. Quantitative metrics described in Sub-Section 4.3 were measured. The sequence of tasks was ordered by resorting on Latin squares' permutations. Finally, user satisfaction and user preference were assessed with a list of statements scored on a 5-point Likert Scale (5 indicates full agreement), while perceived usability and perceived task load were collected by filling out the SUS and NASA-TLX questionnaires, respectively.

5 Results

All data was tested using the Shapiro-Wilk test and although not all metrics followed a normal distribution, all of them presented skewness and kurtosis values within $\pm$ 2 [25]. Statistical significance was tested using three one-way repeated measures ANOVAs, one per parameter space dimension, with Post Hoc pairwise comparison using Least Significant Differences.

Task Completion Time - We extracted the TCTs from the data collected during the study, the results are shown in Figure 6. Amongst the 1-D widgets, *Line* was the fastest method (M = 9.87 s, SD = 4.19 s) and the slowest was *1DSlider* (M = 17.75 s, SD = 10.27 s). There was a statistically significant difference between group means as determined by one-way ANOVA ($F_{(1.42,24.143)}$=12.309, $p < .001$, $\eta^2 = 0.420$) and pairwise comparisons found significant difference between all 3 pairs: *1DSlider* and *Line* (p = .001); *1DSlider* and *LineMap* (p = .005); *Line* and *LineMap* (p = 0.035). Amongst 2-D widgets *Quad* was the fastest (M = 19.04 s, SD = 8.76 s) and *QuadMap* the slowest (M = 28.95 s, SD = 14.58 s) just behind *2DSlider* (M = 28.82 s, SD = 16.90 s). ANOVA determined there was a statistically significant difference ($F_{(2,34)}$=5.588, p = .008, $\eta^2 = 0.247$) and pairwise comparison showed that *2DSlider* and *Quad* (p = .007), as well as *Quad* and *QuadMap* (p = .002) differed significantly. Finally, amongst 3-D widgets *Cube* was the fastest (M = 43.77 s, SD = 20.73 s) and *CubeMap* the slowest (M = 54.87 s, SD = 20.28 s). We found a statistically significant difference ($F_{(2,34)}$=3.493, p = .042, $\eta^2 = 0.170$) and pairwise comparison showed that *Cube* differed significantly from *CubeMap* (p = 0.01).

Selection Error - The measured SEs are shown in Figure 7. Amongst the 1-D widgets, the widget with smallest error was *Line* (M = .011, SD = .009) followed by *LineMap* (M = .012, SD = .012)

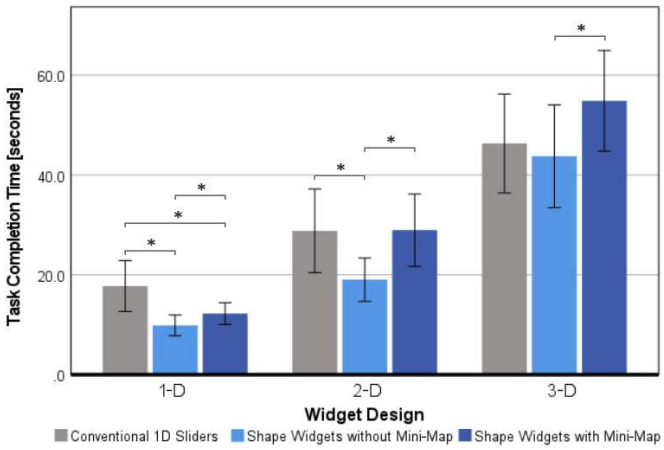

Figure 6: Mean TCT per *WidgetDesign* for 1-D, 2-D, and 3-D exponent parametric spaces. The error bars represent standard error. Horizontal line segments topped with an asterisk (*) denote statistical significant difference.

and the largest error, by a large margin, was *2DSlider* (M = .054, SD = .056). ANOVA analysis found a statistically significant difference ($F_{(1.027,17.454)}$=10.07, p = .005, $\eta^2 = 0.372$) and pairwise comparison showed that *1DSlider* and *Line* (p = .004) as well as *1DSlider* and *LineMap* (p = .007) differed significantly. Amongst 2-D widgets, *QuadMap* had the smallest error (M = .057, SD = .048) and *2DSlider* the largest (M = .159, SD = .182). ANOVA revealed there was a statistically significant effect ($F_{(2,34)}$=3.62, p = .038, $\eta^2 = 0.176$) and pairwise comparison showed a significant difference between *2DSlider* and *QuadMap* (p = 0.16). Amongst 3-D widgets, *Cube* produced the smallest error (M = .158, SD = .122) and *3DSlider* the largest (M = .259, SD = .238). However, the ANOVA analysis was unable to find statistical significance ($F_{(2,34)}$=1.066, p = .355, $\eta^2 = 0.059$).

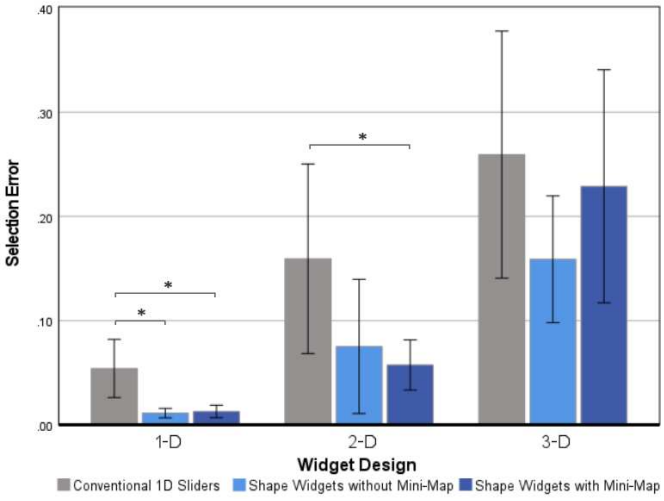

Figure 7: Mean SE per *WidgetDesign* for 1-D, 2-D, and 3-D exponent parametric spaces. The error bars represent standard error. Horizontal line segments topped with an asterisk (*) denote statistical significant difference.

To analyse the qualitative ordinal data such as the score for the SUS and TLX we applied non-parametric Friedman's Test for each

dimension separately (1-D, 2-D, and 3-D exponent parameter space). We then conduct a post-hoc analysis using Wilcoxon signed-rank test to calculate effect size. The reported p-values are Holm-Bonferroni corrected.

System Usability Scale - We calculated the SUS score from the data collected. Amongst the 1-D widgets, *Line* had the greatest mean score (M = 86.11, SD = 11.28), with *1DSlider* (M = 79.0, SD = 11.5) and *LineMap* (M = 78.6, SD = 16.25) having similar inferior scores. Friedman test found statistical significance ($X^2(2)$=9.224, p=.010)) and post hoc tests showed a significant difference between *Line* and *LineMap* (p = .008), as well as *1DSlider* and *Line* (p = .024). Amongst 2-D widgets, similar result was observed with *Quad* coming out on top (M = 82.77, SD = 16.77) and *2DSlider* being the worst mean score (M = 66.39, SD = 22.73). Friedman test found statistical significance ($X^2(2)$=6.2, p=.045)) and post hoc tests showed statistical significance between the pairs *2DSlider* and *Line* (p = .016), and also, *Line* and *LineMap* (p = .004). For the 3-D widgets, we continue to observe the trend where the shape widget with no mini-map (*Cube*) gets the highest SUS score (M = 72.36, SD = 20.14) and the conventional widgets (*3DSlider*) gets the lowest score (M =59.16, SD = 24.47). However, Friedman test showed that no statistical significance was found (p = .33).

Task Load Index - Finally, for the NASA-TLX we observed that VR shape widgets (with and without mini-map) had a slightly lower scores, but after running Friedman test no statistical significance was found ($p \geq .109$).

Regarding user preference ranking, we found that amongst 1-D widgets *Line* was the most preferred by the participants (50%), amongst 2-D shape widgets *Quad* was the most preferred (61%), while *Cube* was the most preferred (44%) of the 3-D shape widgets. The least preferred widgets were *1DSlider* (61%), *2DSlider* (66%) and *3DSlider* (72%).

6 Discussion

Overall, the proposed VR shaped widgets were well received by the participants, even though they were not familiar with supershapes. In general, the performance metrics (TCT and SE), perceived usability, perceived task load, and user preference were better scored next to VR shape widgets without mini-maps, while 1-D sliders presented the lowest scores.

Concerning TCT, the widget shape seems to have a significant effect over task completion times, however this observation is not all-encompassing. For 1-D and 2-D, the VR shape widget design approach clearly leads to shorter times, with the addition of the mini-map the TCT becomes statistically significantly longer but still remains below or equal to the baseline of 1-D Sliders. In the case of 3-D widgets, we found that TCT do not have a significant difference despite the means showing that the mini-map design produces slightly shorter TCTs. Thus, we accept **H1** for 1-D and 2-D widgets but we do not conclude this for 3-D cube widgets as the only valid observation is that the TCT for *CubeMap* is significantly longer than *Cube*. Note that TCT values increase from 1-D to 3-D, which was expectable since higher dimension parameter spaces present more visual information, hence, more content to interact with. Yet, for 2-D and, mainly, 3-D the mini-maps introduced less efficiency. The reason that we see longer TCTs for widgets that include a mini-map is likely due to the increase in cognitive load that comes with the extra functionality to interact with and the increased amount of visual information, leading participants to spend more time reshaping their selection inside two distinct interactive spaces. We expected this trade-off to come at the expense of selection tasks with finer control and improved accuracy.

As for selection accuracy, we notice that a significant increase appears when comparing the conventional widgets *1DSlider* and *2DSlider* to their shape widget counterparts, both with and without the inclusion of a mini-map (i.e., *Line*, *LineMap*, *Quad*, and *QuadMap*), which leads us to accept **H2** for both 1-D and 2-D widgets dimensions. Once again, despite the lack of statistical significance, we do find the same trend with the 3-D widgets but we fall short of being able to accept **H2** in this case. This might be due to the small test sample size or the high variance found in the data collected. However, the non-linear behaviour of the supershape formula (Equation 1) may have affected the SE when target shapes present either $n_1 > 2$ or $n_{2,3} > 2$ as the formula can render visually identical shapes for different exponent parameter values, thus, leading participants to select one solution from several solutions that look alike but have distinct exponent values. To attain a more representative SE metric, we could consider a metric based not on the difference between exponent parameters but rather on the differences between 2-D signals (e.g., dynamic time warping), yet cognitive science studies report that when performing visual similarity-judgment task, our perception of shapes is not based on differences, but on similarity [36]. So, greater attention needs to be given on how to formulate a representative SE metric, possibly one that combines exponent values, 2-D signal processing and perception metrics.

Unexpectedly, we did not observe a significant effect in SE for shape widget including the mini-map. According to participant feedback, the thumbnails paradigm is not appropriate for fine-tuning at the scale. This is due to the fact that spotting visual differences between shapes that are too alike becomes increasingly harder when this difference is so reduced. Users would sometimes mistakenly select a neighbouring shape and become frustrated at the fact that it did not produce the expected change. From these observations we reject **H3** and conclude that the increase in TCT that comes with implementing a mini-map with a discrete set of solutions requires further design iterations.

As for perceived usability, the analysis of SUS scores were largely inconclusive. We saw a significant effect for 1-D and 2-D dimensions, but not 3-D. In spite of this, our means revealed VR shape widgets without mini-maps to be most well scored in terms of usability across the board. Despite the lack of statistical significance, which does not support **H5**, participant feedback and user preferences painted a favorable image for these shape widgets.

Finally, we expected that the VR shape widgets would imply higher perceived task load. However, despite presenting more visual information and requiring higher physical exertion, this assumption was not supported by the results of the analysis to TLX where we observed no significant effect and the means actually presented an optimistic perception in that the scores for shape widgets were overall lower. Thus, we can safely reject **H4**.

7 Conclusions and Future Work

In this work, we designed novel VR shape widgets for probing and selecting supershapes. We conducted a user study to compare the VR shape widgets with conventional VR 1-D sliders. Our findings indicate that (i) the proposed VR shape widgets are effective, more efficient, and promote a more natural interaction when compared to conventional VR 1-D sliders; (ii) the VR shape widget without mini-maps are more appropriate for probing and selecting supershapes, being more accurate and less time-consuming approach for supershape selection when compared to conventional 1-D sliders or when resorting to mini-maps; and (iii) more importantly, we found that the proposed VR shape widget are effective and usable for novice users without prior knowledge in supershapes.

Finally, despite our efforts in pandemic times we only tested our VR widgets next to 18 participants. Even though a greater number participants would provide more solid statistical evidence to support the reported findings, our initial concepts of VR shape widgets were validated from the collected feedback and point towards future work on parametric modeling with supershapes in VR. In particular, we

aim to include the VR shape widgets in a VR 3D modeling tool that supports nature patterns as 3D primitives to model organic objects, specially those with many details of complex shapes [50]. We also intend to conduct an in-depth user study next to professionals such as digital artists, 3D modelers and architects that would be asked to perform several shape exploration tasks to properly validate the computational creativity side of the VR shape widgets. Still on exploratory tasks, we aim to build a comprehensive supershape taxonomy that could provide relevant shape cues on how handle adjustments affect shape features, and we also intend to verify how haptic techniques can be used to encode shape information through vibration signatures allowing users to better distinguish two supershapes or identify specific class of supershapes.

ACKNOWLEDGMENTS

This research was supported by the Fundação para a Ciência e a Tecnologia through grant UIDB/50021/2020.

REFERENCES

[1] Google Blocks, 2021. https://vr.google.com/blocks/.

[2] Gravity Sketch, 2021. https://www.gravitysketch.com/.

[3] Supershapes - Unreal Market Place, 2021. https://www.unrealengine.com/marketplace/en-US/product/supershapes.

[4] VRSketch, 2021. https://vrsketch.eu/.

[5] M. Alger. Visual design methods for virtual reality. *Ravensbourne. http://aperturesciencellc.com/vr/VisualDesignMethodsforVR_MikeAlger.pdf*, 2015.

[6] F. Babaei, M. Javidnasab, and A. Rezaei. Supershape nanoparticle plasmons. *Plasmonics*, 13(4):1491–1497, Aug 2018. doi: 10.1007/s11468-017-0655-5

[7] B. Bach, P. Dragicevic, D. Archambault, C. Hurter, and S. Carpendale. A descriptive framework for temporal data visualizations based on generalized space-time cubes. *Comput. Graph. Forum*, 36(6):36–61, Sept. 2017. doi: 10.1111/cgf.12804

[8] V. Basile, M. Grande, V. Marrocco, D. Laneve, S. Petrignani, F. Prudenzano, and I. Fassi. Design and manufacturing of super-shaped dielectric resonator antennas for 5g applications using stereolithography. *IEEE Access*, 8:82929–82937, 2020. doi: 10.1109/ACCESS.2020.2991358

[9] T. V. Bouwel. DesignSpace VR, 2021. http://www.designspacevr.org/.

[10] D. A. Bowman, E. Kruijff, J. J. LaViola, and I. Poupyrev. An introduction to 3-d user interface design. *Presence: Teleoper. Virtual Environ.*, 10(1):96–108, Feb. 2001. doi: 10.1162/105474601750182342

[11] I. Caetano, L. Santos, and A. Leitão. Computational design in architecture: Defining parametric, generative, and algorithmic design. *Frontiers of Architectural Research*, 9(2):287–300, 2020. doi: 10.1016/j.foar.2019.12.008

[12] W. Chen and M. Fuge. Béziergan: Automatic generation of smooth curves from interpretable low-dimensional parameters. *arXiv preprint arXiv:1808.08871*, 2018.

[13] W. Chen, M. Fuge, and J. Chazan. Design Manifolds Capture the Intrinsic Complexity and Dimension of Design Spaces. *Journal of Mechanical Design*, 139(5), 03 2017. 051102. doi: 10.1115/1.4036134

[14] K. Danyluk, B. Ens, B. Jenny, and W. Willett. *A Design Space Exploration of Worlds in Miniature*. Association for Computing Machinery, New York, NY, USA, 2021.

[15] R. de Klerk, A. M. Duarte, D. P. Medeiros, J. P. Duarte, J. Jorge, and D. S. Lopes. Usability studies on building early stage architectural models in virtual reality. *Automation in Construction*, 103:104–116, 2019. doi: 10.1016/j.autcon.2019.03.009

[16] T. De Smedt, L. Lechat, and W. Daelemans. Generative art inspired by nature, using nodebox. In *Proceedings of the 2011 International Conference on Applications of Evolutionary Computation - Volume Part II*, EvoApplications'11, p. 264–272. Springer-Verlag, Berlin, Heidelberg, 2011.

[17] S. M. Feeman, L. B. Wright, and J. L. Salmon. Exploration and evaluation of cad modeling in virtual reality. *Computer-Aided Design and Applications*, 15(6):892–904, 2018. doi: 10.1080/16864360.2018.1462570

[18] J.-D. Fekete. The infovis toolkit. In *Proceedings of the IEEE Symposium on Information Visualization*, INFOVIS '04, p. 167–174. IEEE Computer Society, USA, 2004.

[19] J. Ferreira, D. Mendes, R. Nóbrega, and R. Rodrigues. Immersive multimodal and procedurally-assisted creation of vr environments. In *2021 IEEE Conference on Virtual Reality and 3D User Interfaces Abstracts and Workshops (VRW)*, pp. 30–37, 2021. doi: 10.1109/VRW52623.2021.00012

[20] Y. Fougerolle, A. Gribok, S. Foufou, F. Truchetet, and M. Abidi. Boolean operations with implicit and parametric representation of primitives using r-functions. *IEEE Transactions on Visualization and Computer Graphics*, 11(5):529–539, 2005. doi: 10.1109/TVCG.2005.72

[21] Y. Fougerolle, A. Gribok, S. Foufou, F. Truchetet, and M. Abidi. Rational supershapes for surface reconstruction - art. no. 63560m. *Proceedings of SPIE - The International Society for Optical Engineering*, 6356, 05 2007. doi: 10.1117/12.736916

[22] Y. Fougerolle, F. Truchetet, and J. Gielis. Potential fields of self intersecting gielis curves for modeling and generalized blending techniques. In J. Gielis, P. E. Ricci, and I. Tavkhelidze, eds., *Modeling in Mathematics*, pp. 67–81. Atlantis Press, Paris, 2017.

[23] Y. D. Fougerolle, J. Gielis, and F. Truchetet. A robust evolutionary algorithm for the recovery of rational gielis curves. *Pattern Recogn.*, 46(8):2078–2091, Aug. 2013. doi: 10.1016/j.patcog.2013.01.024

[24] G. Garrofé, C. Parés, A. Gutiérrez, C. Ruiz, G. Serra, and D. Miralles. Virtual haptic system for shape recognition based on local curvatures. In N. Magnenat-Thalmann, V. Interrante, D. Thalmann, G. Papagiannakis, B. Sheng, J. Kim, and M. Gavrilova, eds., *Advances in Computer Graphics*, pp. 41–53. Springer International Publishing, Cham, 2021.

[25] D. George and P. Mallery. *SPSS® for Windows® step by step: A simple guide and reference (9.0 Update)*. Allyn & Bacon, Boston, 1999.

[26] J. Gielis. A generic geometric transformation that unifies a wide range of natural and abstract shapes. *American Journal of Botany*, 90(3):333–338, 2003. doi: 10.3732/ajb.90.3.333

[27] J. Gielis. *The Geometrical Beauty of Plants*. Atlantis Press, 2017.

[28] J. Gielis, E. Bastiaens, T. Krikken, A. Kiefer, and M. de Blochouse. Variational superformula curves for 2d and 3d graphic arts. In *ACM SIGGRAPH 2004 Posters*, SIGGRAPH '04, p. 5. Association for Computing Machinery, New York, NY, USA, 2004. doi: 10.1145/1186415.1186421

[29] J. Gielis and B. Beirinckx. Superformula solutions for 3d graphic arts and cad/cam. In *ACM SIGGRAPH 2004 Posters*, SIGGRAPH '04, p. 4. Association for Computing Machinery, New York, NY, USA, 2004. doi: 10.1145/1186415.1186420

[30] J. Gielis, P. Shi, B. Beirinckx, D. Caratelli, and P. E. Ricci. Lamé-gielis curves in biology and geometry. In *Proceedings of the Conference Riemannian Geometry and Applications*, RIGA 2021, 2021.

[31] S. G. Hart. Nasa-task load index (nasa-tlx); 20 years later. *Proceedings of the Human Factors and Ergonomics Society Annual Meeting*, 50(9):904–908, 2006. doi: 10.1177/154193120605000909

[32] X. He, Y. Tao, Q. Wang, and H. Lin. Multivariate spatial data visualization: a survey. *Journal of Visualization*, 22(5):897–912, Oct 2019. doi: 10.1007/s12650-019-00584-3

[33] L. Hirsch, B. Rossmy, and A. Butz. Shaping concrete for interaction. In *Proceedings of the Fifteenth International Conference on Tangible, Embedded, and Embodied Interaction*, TEI '21. Association for Computing Machinery, New York, NY, USA, 2021. doi: 10.1145/3430524.3440625

[34] J. Jerald. *The VR Book: Human-Centered Design for Virtual Reality*. Morgan /&; Claypool Publishers, 2015.

[35] Y. Koyama, I. Sato, and M. Goto. Sequential gallery for interactive visual design optimization. *ACM Trans. Graph.*, 39(4), July 2020. doi: 10.1145/3386569.3392444

[36] H. Lee Masson, J. Bulthé, H. P. Op de Beeck, and C. Wallraven. Visual and Haptic Shape Processing in the Human Brain: Unisensory Processing, Multisensory Convergence, and Top-Down Influences. *Cerebral Cortex*, 26(8):3402–3412, 07 2016. doi: 10.1093/cercor/bhv170

[37] C. Liang, G. Baciu, J. Zhang, E. C. L. Chan, and G. Li. Footprint-

profile sweep surface: A flexible method for realtime generation and rendering of massive urban buildings. In *Proceedings of the 17th ACM Symposium on Virtual Reality Software and Technology*, VRST '10, p. 151–158. Association for Computing Machinery, New York, NY, USA, 2010. doi: 10.1145/1889863.1889896

[38] J. Liu, A. Prouzeau, B. Ens, and T. Dwyer. Design and evaluation of interactive small multiples data visualisation in immersive spaces. In *2020 IEEE Conference on Virtual Reality and 3D User Interfaces (VR)*, pp. 588–597, March 2020. doi: 10.1109/VR46266.2020.00081

[39] D. S. Lopes, R. K. dos Anjos, and J. A. Jorge. Assessing the usability of tile-based interfaces to visually navigate 3-d parameter domains. *International Journal of Human-Computer Studies*, 118:1 – 13, 2018. doi: 10.1016/j.ijhcs.2018.05.005

[40] A. Marsh. Andrew Marsh - Supershapes WebGL App, 2021. `http://andrewmarsh.com/software/supershapes-web/`.

[41] J. Matejka, M. Glueck, T. Grossman, and G. Fitzmaurice. The effect of visual appearance on the performance of continuous sliders and visual analogue scales. In *Proceedings of the 2016 CHI Conference on Human Factors in Computing Systems*, CHI '16, p. 5421–5432. Association for Computing Machinery, New York, NY, USA, 2016. doi: 10.1145/2858036.2858063

[42] M. Matsuura. Gielis' superformula and regular polygons. *Journal of Geometry*, 106(2):383–403, Jul 2015. doi: 10.1007/s00022-015-0269-z

[43] J. K. Moo-Young, A. Hogue, and V. Szkudlarek. Virtual materiality: Realistic clay sculpting in vr. In *Extended Abstracts of the 2021 Annual Symposium on Computer-Human Interaction in Play*, CHI PLAY '21, p. 105–110. Association for Computing Machinery, New York, NY, USA, 2021. doi: 10.1145/3450337.3483475

[44] R. J. Preen and L. Bull. ˙ *Evolutionary Intelligence*, 7(3):155–167, Nov 2014. doi: 10.1007/s12065-014-0116-4

[45] M. Rietzler, F. Geiselhart, J. Frommel, and E. Rukzio. *Conveying the Perception of Kinesthetic Feedback in Virtual Reality Using State-of-the-Art Hardware*, p. 1–13. Association for Computing Machinery, New York, NY, USA, 2018.

[46] E. Rosales, J. Rodriguez, and A. SHEFFER. Surfacebrush: From virtual reality drawings to manifold surfaces. *ACM Trans. Graph.*, 38(4), July 2019. doi: 10.1145/3306346.3322970

[47] P. Shi, D. Ratkowsky, and J. Gielis. The generalized gielis geometric equation and its application. *Symmetry*, 12:645, 04 2020. doi: 10.3390/sym12040645

[48] F. Tian, Y. Wang, H. S. Sandhu, J. Gielis, and P. Shi. Comparison of seed morphology of two ginkgo cultivars. *Journal of Forestry Research*, 31(3):751–758, Jun 2020. doi: 10.1007/s11676-018-0770-y

[49] S. Voisin, M. A. Abidi, S. Foufou, and F. Truchetet. Genetic algorithms for 3d reconstruction with supershapes. In *2009 16th IEEE International Conference on Image Processing (ICIP)*, pp. 529–532, Nov 2009. doi: 10.1109/ICIP.2009.5413905

[50] F. Zhang, Z. Liu, Z. Cheng, O. Deussen, B. Chen, and Y. Wang. Mid-air finger sketching for tree modeling. In *2021 IEEE Virtual Reality and 3D User Interfaces (VR)*, pp. 826–834, 2021. doi: 10.1109/VR50410.2021.00110